Supporting information

A Novel Compositional-Gradient Hierarchical ZnS/GeS_2 Heterojunction Nanorods for High-Rate and Durable Sodium Storage

Jun Zhao,[a] *Huaixin, Wei,*[a]* *Wenqin Bian,*[b] *Shujue Gu,*[b] *Hao Yang,*[b] *Yun Cheng,*[c]* *Liang Cao,*[b]*

[a] J. Zhao and Prof. H. Wei

School of Chemistry and life Sciences

Suzhou University of Science and Technology

Suzhou, Jiangsu 215009, P. R. China

E-mail: hxwei@usts.edu.cn

[b] Y. Xue, Y. Wang, X. Cui, L. Cao, Prof. H. Geng

School of Materials Engineering

Suzhou University of Technology

Changshu, Jiangsu 215500, P. R. China

Email: liangcao@szut.edu.cn

[c] Y. Cheng

Guangdong Saffien New Materials CO., LTD，

E-mail: chengerr@126.com

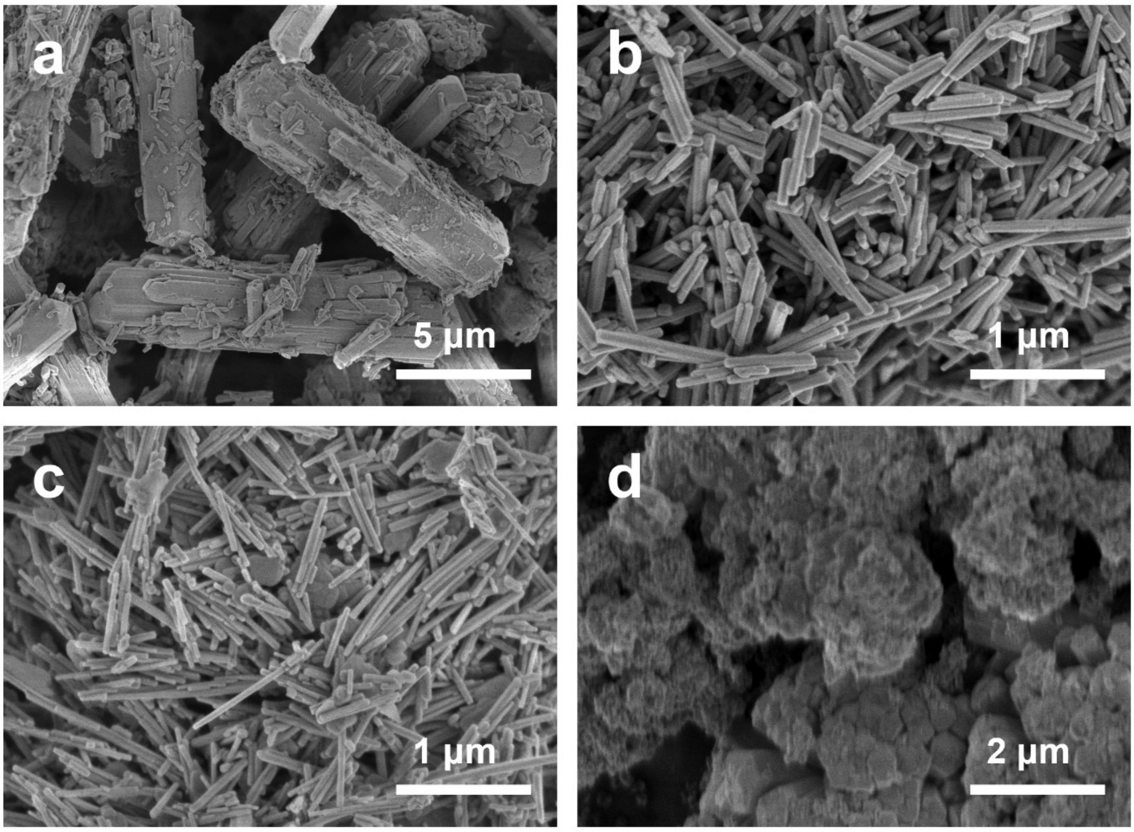

Fig. S1. (a) SEM image of the precursor obtained at pH 8, (b) Precursor prepared at pH 9, (c) Sample synthesized at pH 10, (d) Sample prepared with excessive NH_3.

At low pH, no solid precursor forms; when the pH is moderately increased by adding a small amount of $NH_3 \cdot H_2O$, uniform nanorods are obtained, whereas excessively high pH disrupts the growth process and leads to fragmented and unstable rod structures.

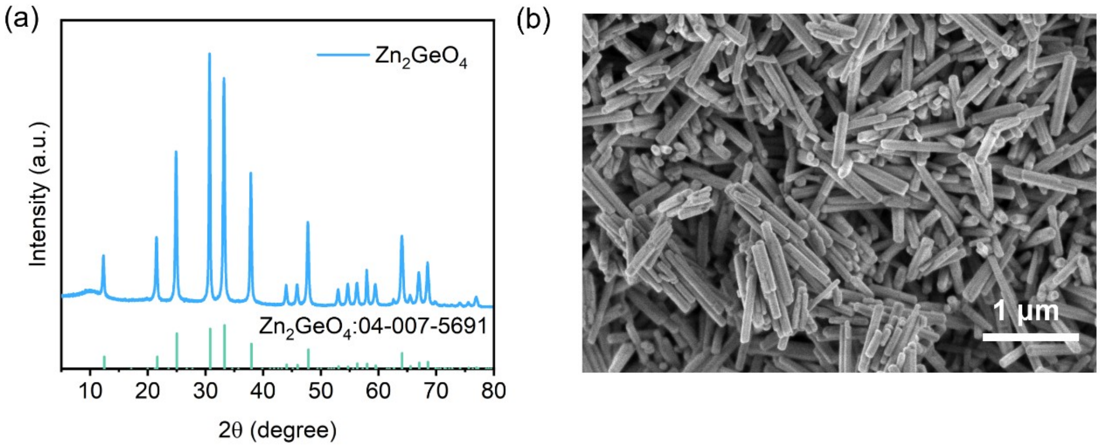

Fig. S2. Physical characterizations of Zn_2GeO_4 precursor. (a) XRD patterns and (b) SEM image.

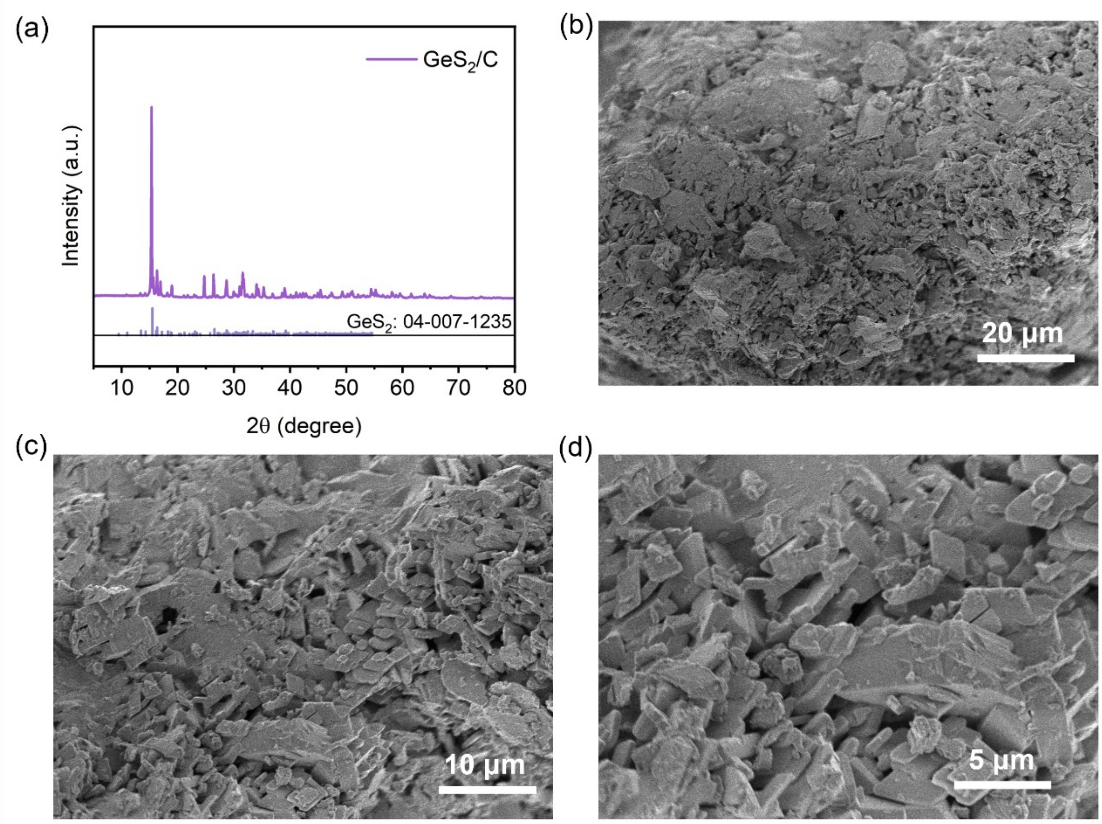

Fig. S3. Physical characterizations of pure GeS_2/C composite. (a) XRD patterns and (b-d) SEM image.

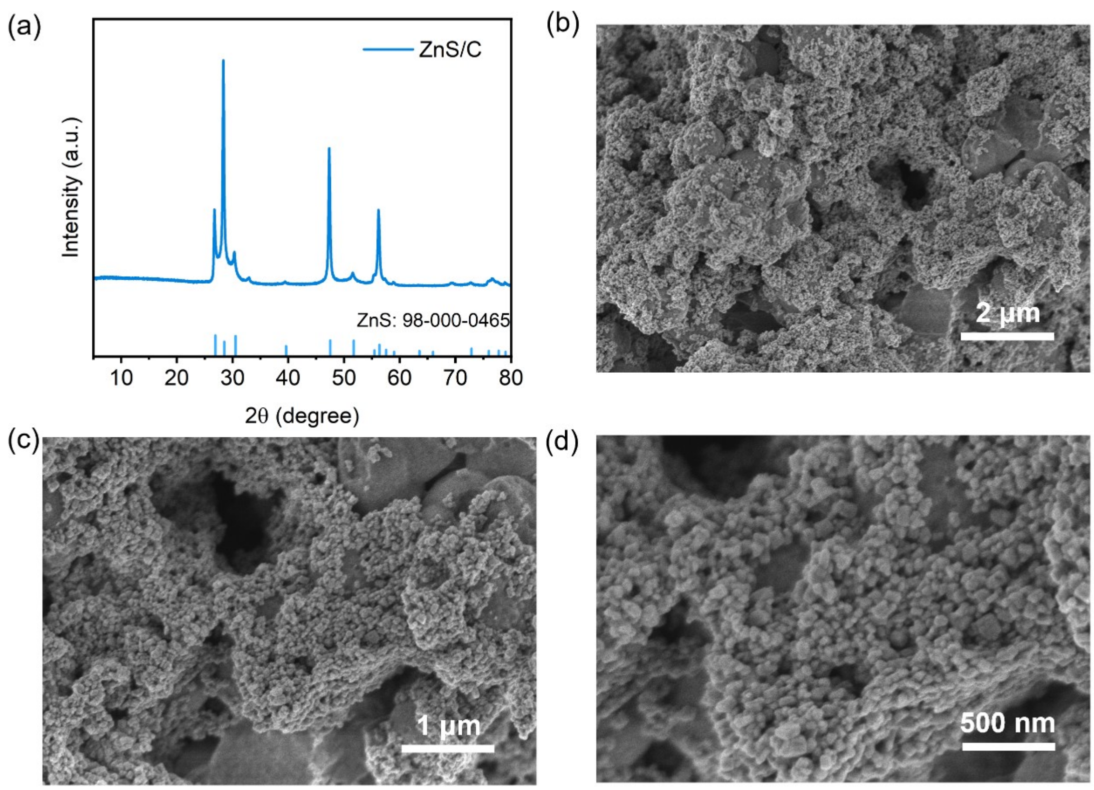

Fig. S4. Physical characterizations of pure ZnS/C composite. (a) XRD patterns and (b-d) SEM image.

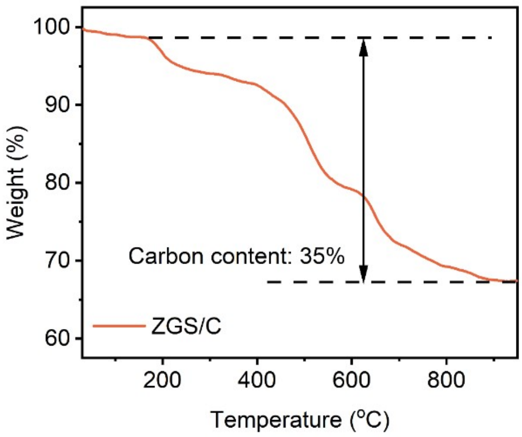

Fig S5. TGA curves of ZGS/C composites.

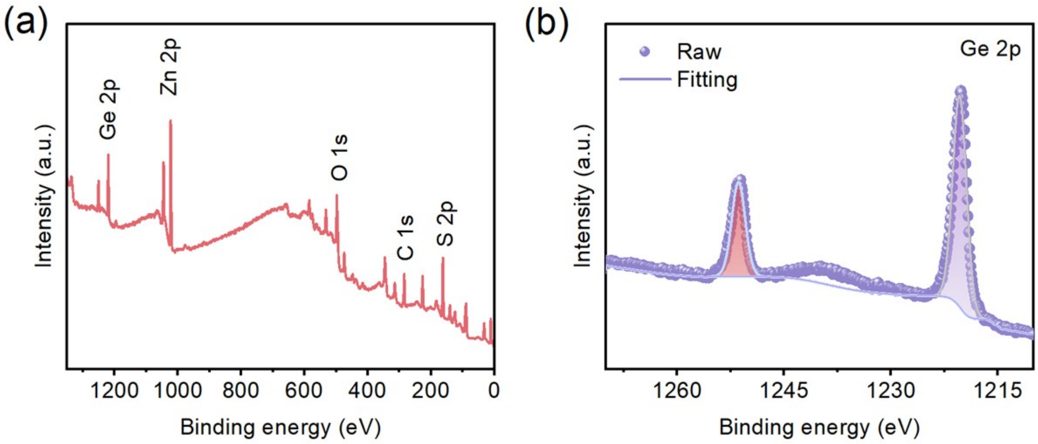

Fig. S6. XPS analysis of ZGS/C composite. (a) Survey spectrum, and (b) Zn 2p high-resolution spectrum.

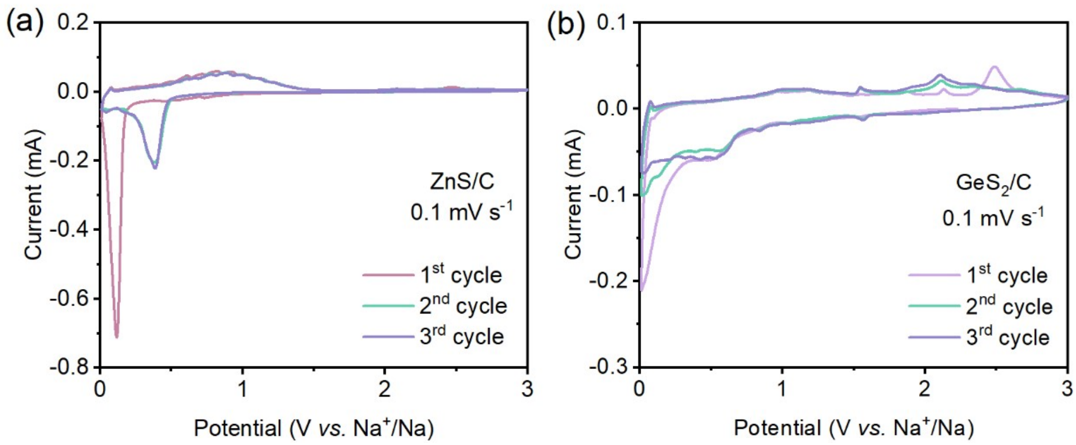

Fig. S7. Initial three CV curves of ZnS/C and GeS_2/C electrodes at 0.1 mV s^{-1}.

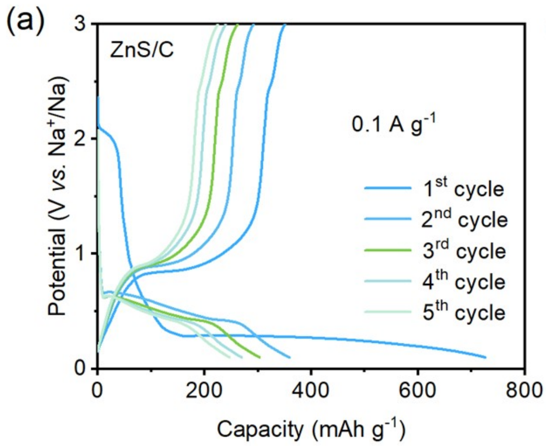

Fig. S8. Initial five discharge-charge curves at 0.1 A g^{-1}, (a) ZnS/C and (b)GeS_2/C electrodes.

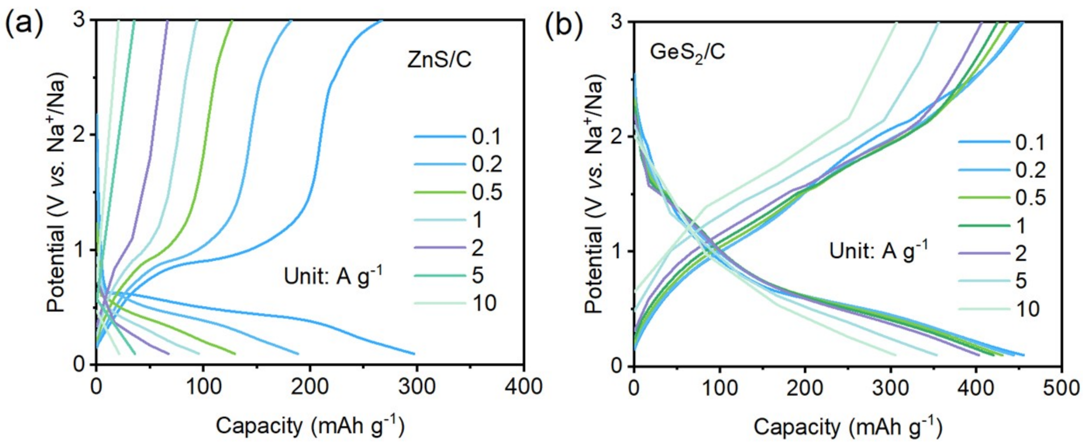

Fig. S9. The discharge-charge curves of (a) ZnS/C and (b) GeS_2/C electrodes at various current rates from 0.1 to 10 A g^{-1}.

Table S1. Comparison of reversible capacity and cycling lifespan with reported ZnS or GeS_2-based anode in SIBs.

Sample	**Current ($A\ g^{-1}$)**	**Capacity ($mAh\ g^{-1}$)**	**Cycle number (n)**	**References**
NiS/ZnS@C-AT	2	404.5	1900	[1]
ZnS/Co	2	557	1500	[2]
ZnS/NC	1	244.1	900	[3]
N, S-HC@ZnS	2	308.33	1000	[4]
ZnS NSs@rGO	0.5	634.6	1000	[5]
ZSG	1	174.3	1000	[6]
$ZnIn_2S_4$	5	394.3	500	[7]
2D Ultrathin GeS_2 Nanosheets	10	515	2000	[8]
GeS_2/Graphene	2	371	800	[9]
Carbon confined GeS_2	0.1	266.5	500	[10]
Amorphous structured GeS_2	10	512.8	1000	[11]
This work	10	446	3000	

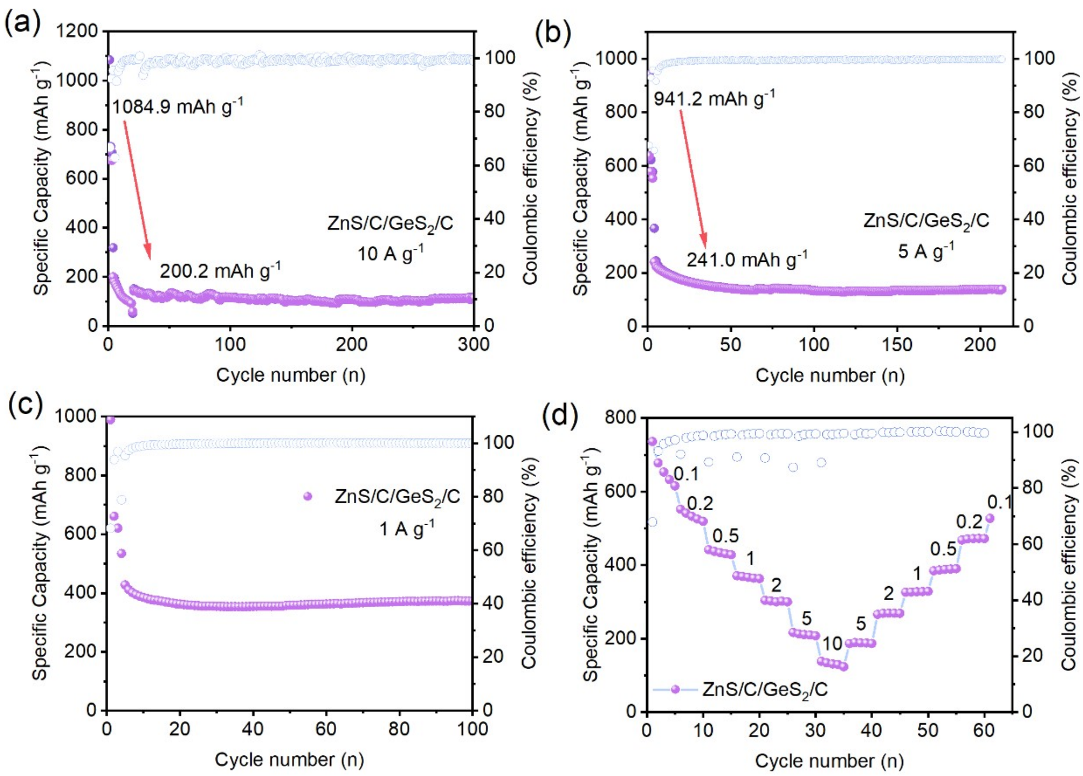

Fig S10. (a-c) Long-term cycling, and (d) rate capability of ZnS/C/GeS_2/C electrode.

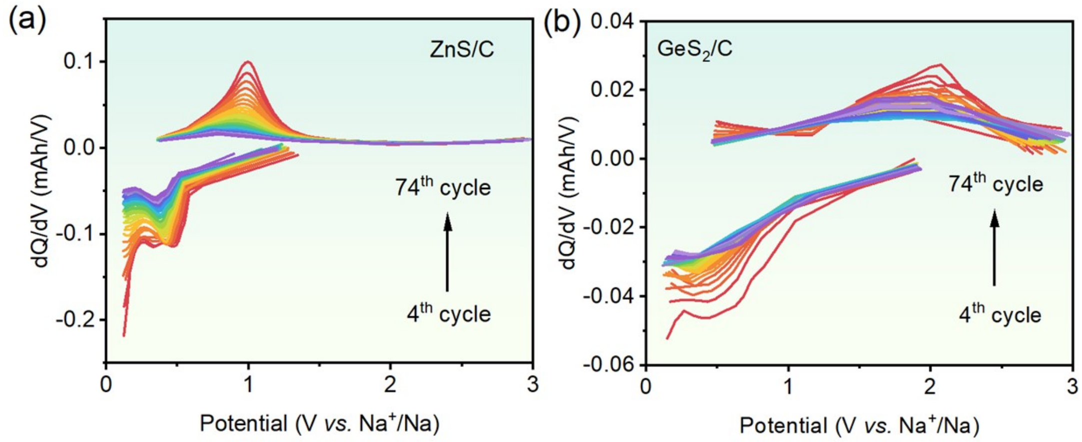

Fig. S11. dQ/dV curves of (a) ZnS/C and (b) GeS_2/C electrodes at 1.0 A g^{-1}.

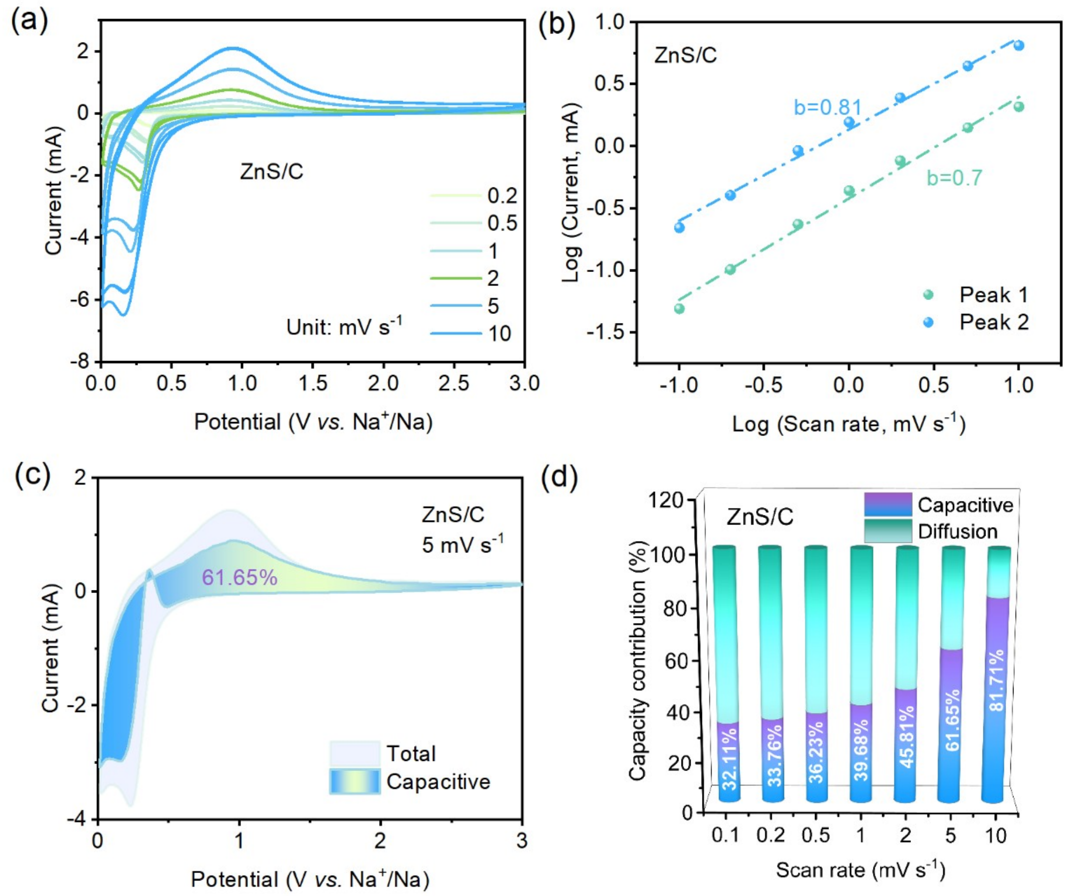

Fig. S12. Reaction kinetics of ZnS/C electrode. (a) Various CV curves at different scan rates from 0.2 to 10 mV s^{-1}. (b) Plot of log (scan rate) *vs.* log (peak current) from CV curves. (c) Capacitive contribution in the CV curves of ZnS/C electrode at 5 mV s^{-1}. (d) Capacitive contribution of ZnS/C at various scan rates.

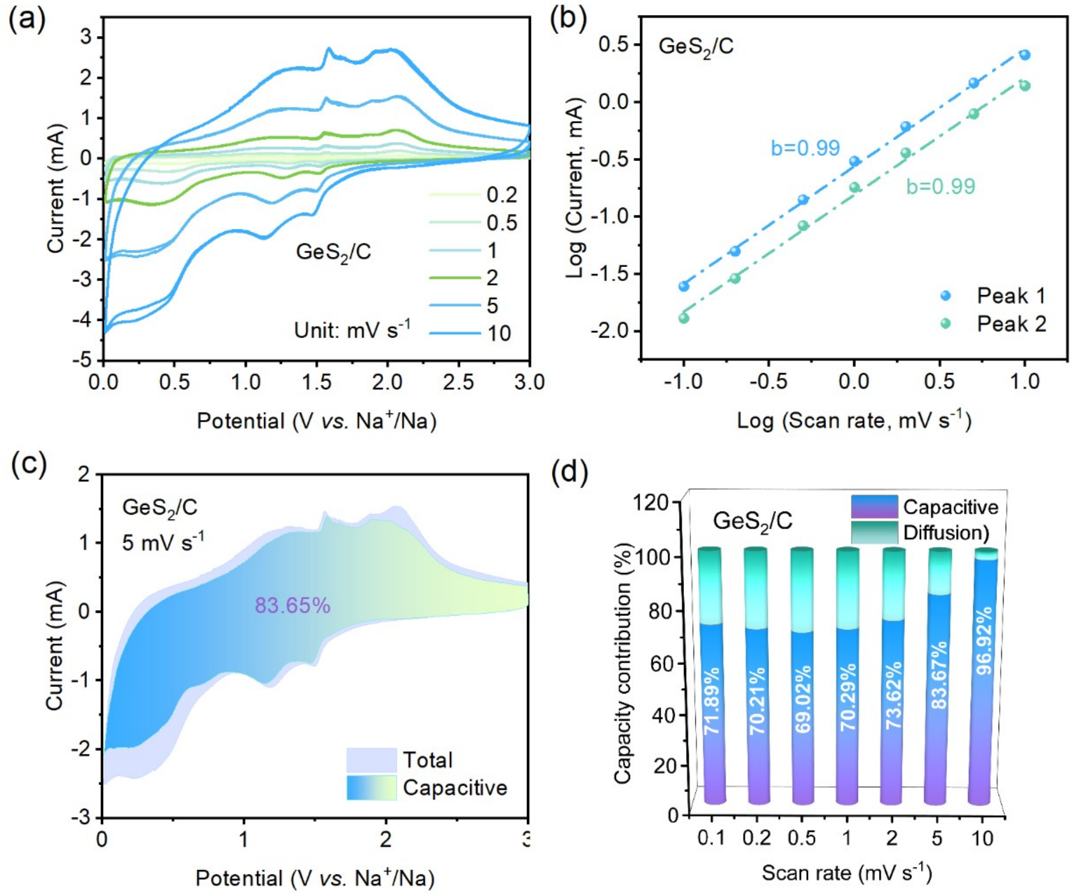

Fig. S13. Reaction kinetics of GeS_2/C electrode. (a) Various CV curves at different scan rates from 0.2 to 10 mV s^{-1}. (b) Plot of log (scan rate) *vs.* log (peak current) from CV curves. (c) Capacitive contribution in the CV curves of GeS_2/C electrode at 5 mV s^{-1}. (d) Capacitive contribution of GeS_2/C at various scan rates.

Table S2. The corresponding data of activation energy in Fig. 4g.

1000/T (k^{-1})	ZGS/C	ZnS/C	GeS_2/C
3.35	-1.73	-2.45	-2.62
3.30	-1.69	-2.49	-2.60
3.25	-1.65	-2.39	-2.59
3.19	-1.56	-2.34	-2.57
3.14	-1.49	-2.18	-1.93

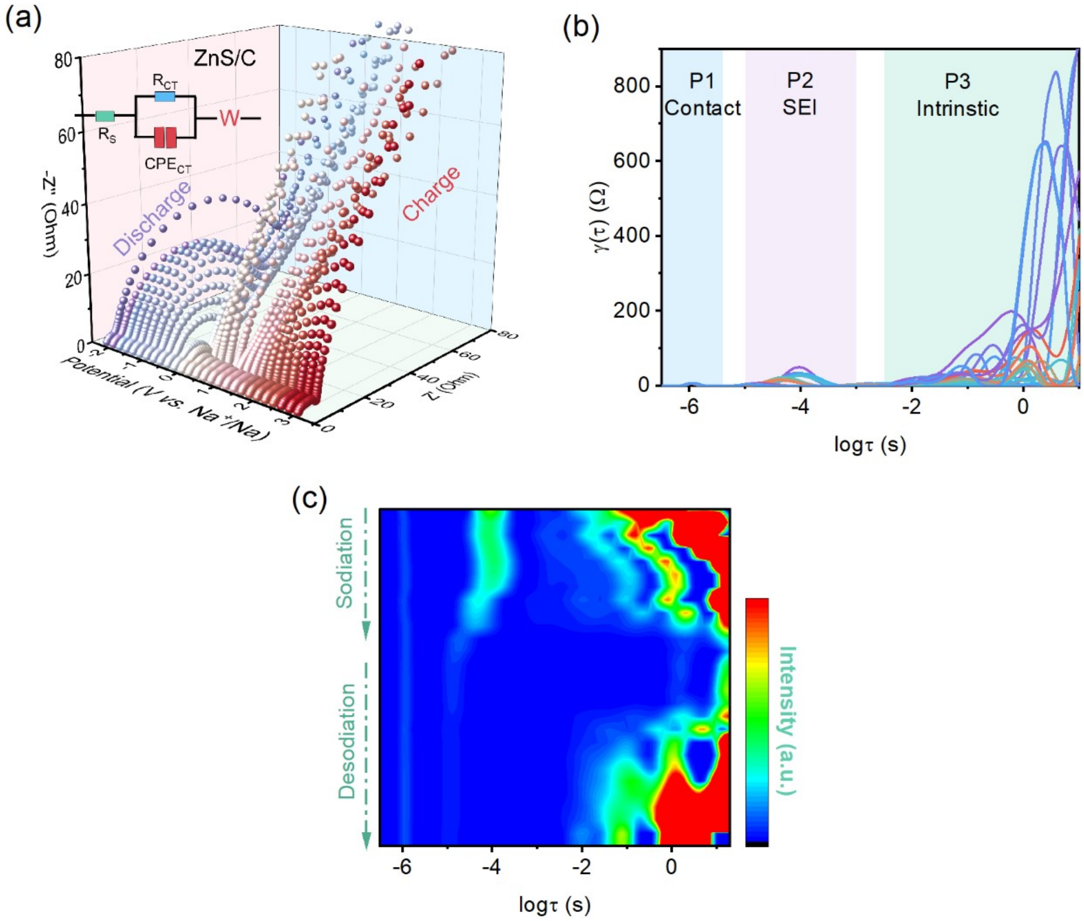

Fig. S14. Characterization of Na^+ transport in ZnS/C half-cell. (a) In-situ EIS curves. (b) DRT curves and (c) their contour map.

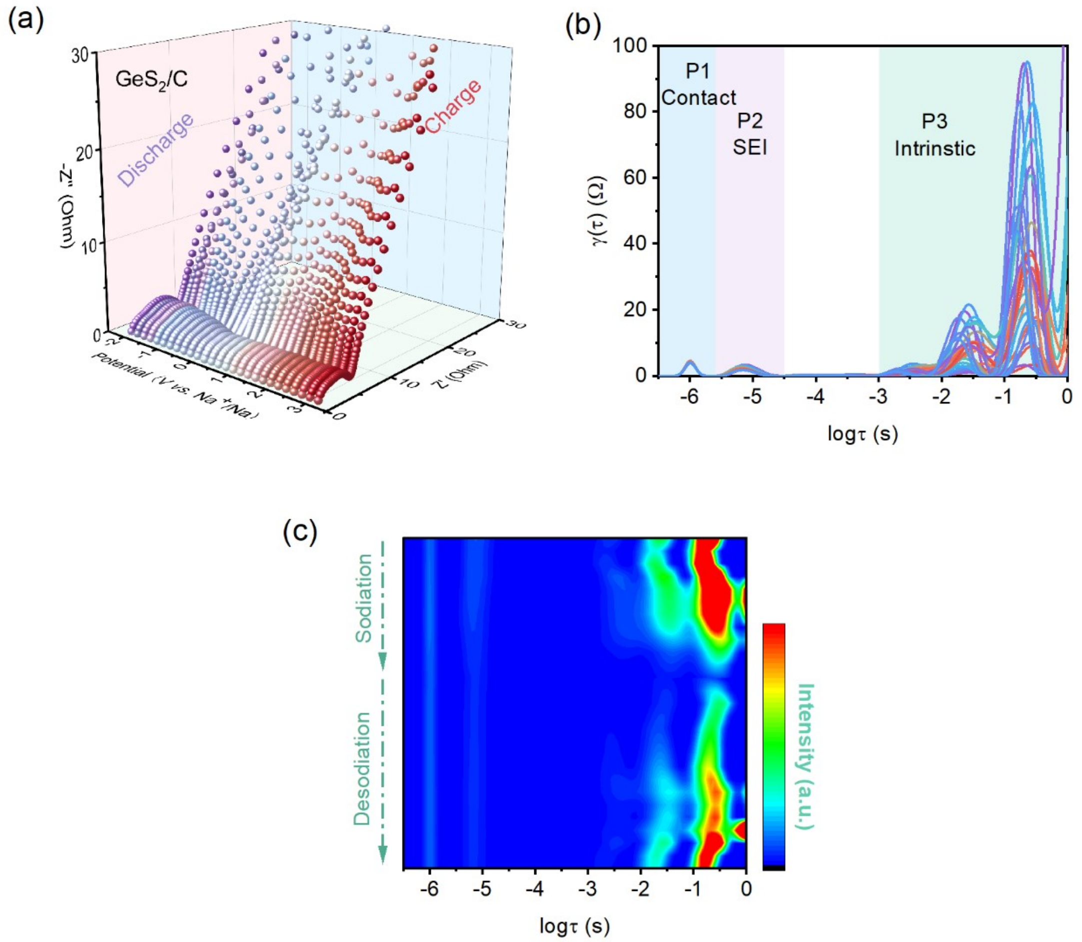

Fig. S15. Characterization of Na^+ transport in GeS_2/C half-cell. (a) In-situ EIS curves. (b) DRT curves and (c) their contour map.

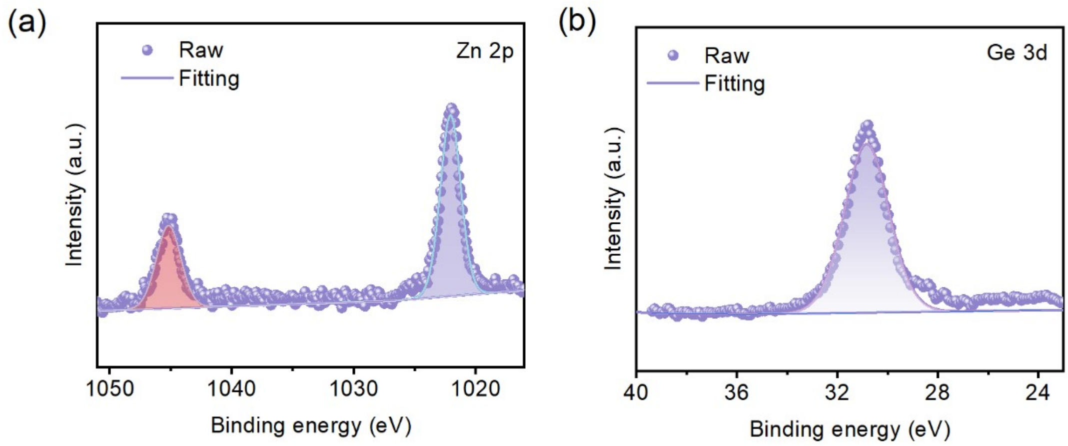

Fig. S16. XPS spectra of ZGS/C electrode after 50 cycles at 1 A g^{-1}: (a) Zn 2p high-resolution spectra and (b) Ge 3d high-resolution spectra.

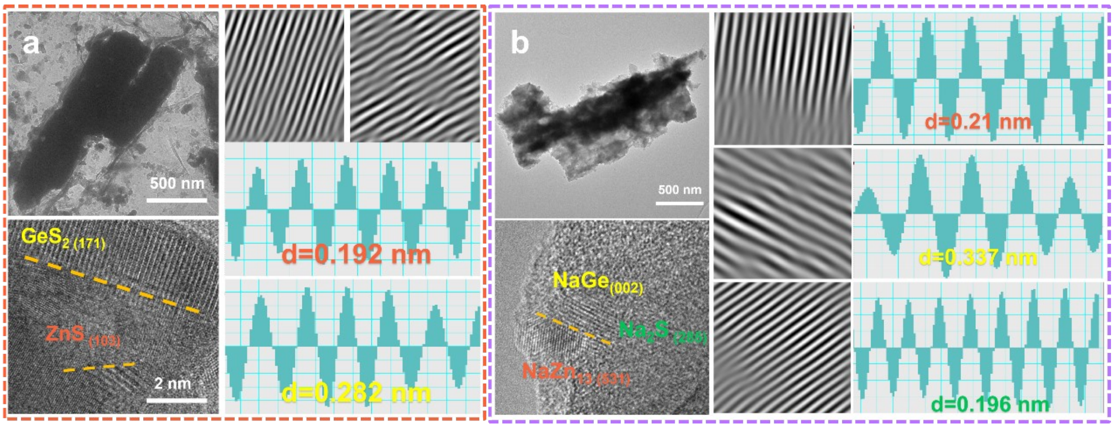

Fig S17. (a, b) HRTEM images of the ZGS/C electrode at the charged state and discharged states.

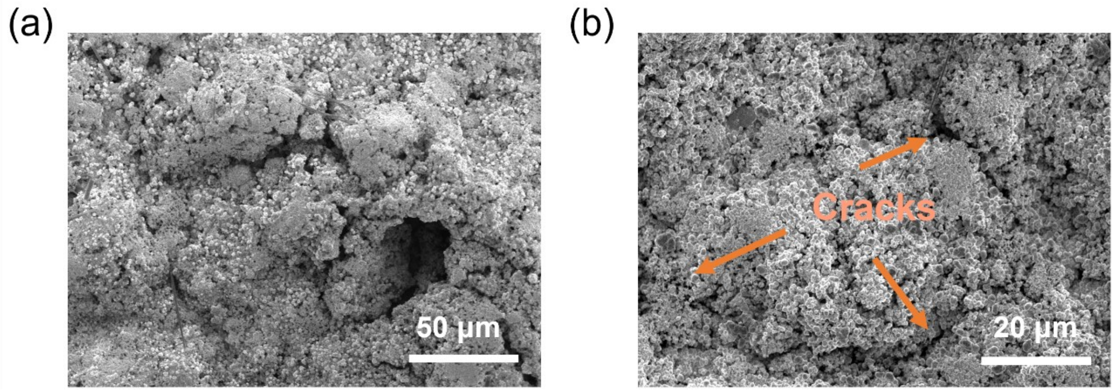

Fig. S18. (a,b) SEM images of ZnS/C electrode after 50 cycles at 1 A g^{-1}.

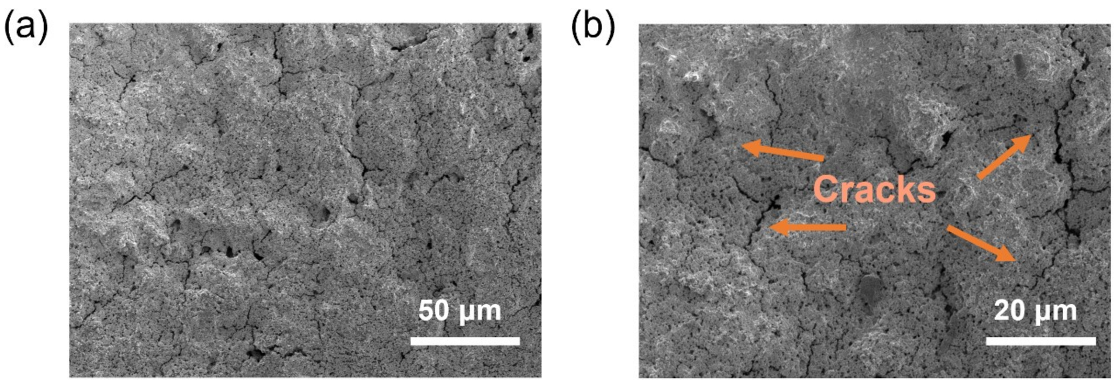

Fig. S19. (a,b) SEM images of GeS_2/C electrode after 50 cycles at 1 A g^{-1}.

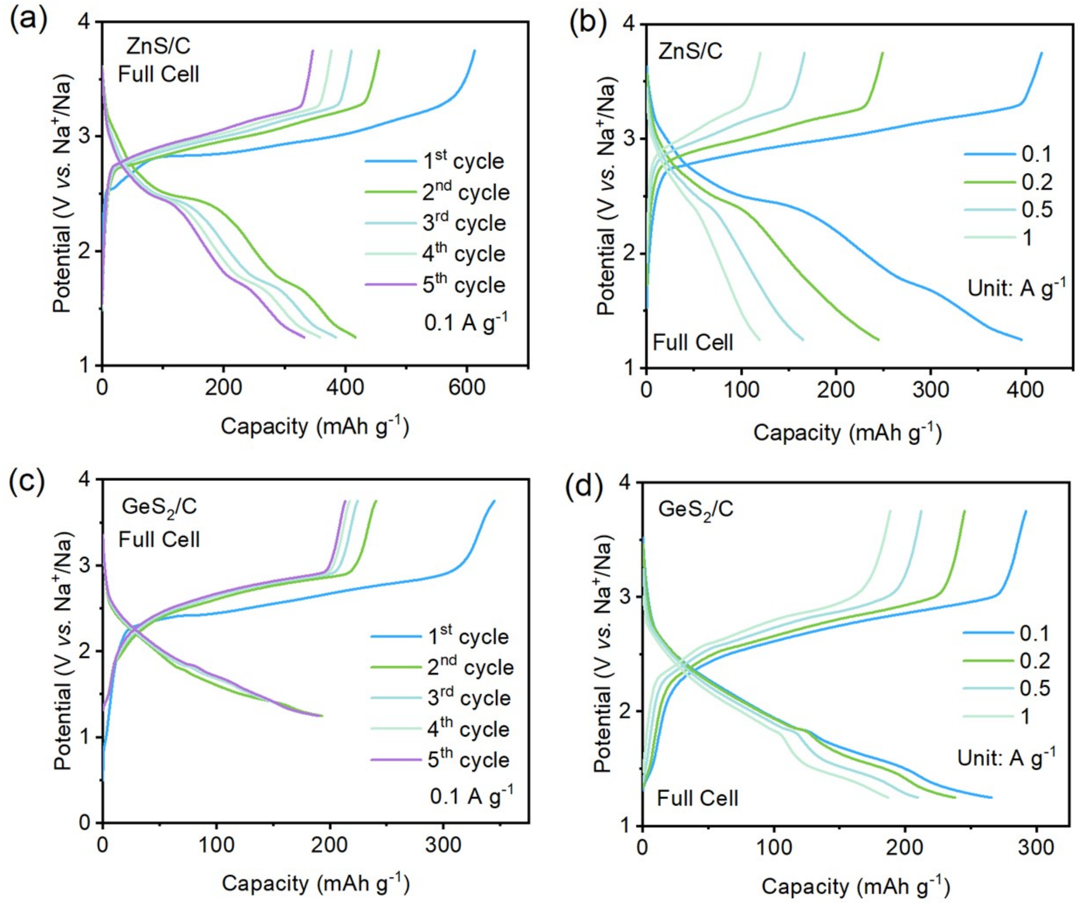

Fig. S20. (a,c) Initial five discharge-charge curves of ZnS/C and GeS_2/C electrodes at 0.1 A g^{-1}. (b,d) The discharge-charge curves at various current rates from 0.1 to 1 Ag^{-1} of ZnS/C and GeS_2/C electrodes.

References

[1] J. Wang, J. Fan, M. Fan, X. Yue, J. Zhang, Z. Liu, Z. Xie, Q. Zhao, A. Abudula, G. Guan, MOF derived NiS/ZnS heterostructure enhancing the electrochemical kinetics for sodium ion batteries, J. Power Sources, 2025, **626**, 235803, DOI 10.1016/j.jpowsour.2024.235803.

[2] H. Zhang, D. Yu, F. Yuan, Y. Jin, L. Song, M. Zhang, H. Zheng, Heterostructured ZnS/Co embedded in pinecone-like N/S-doped carbon for efficient sodium/lithium storage, Chem. Eng. J., 2024, **489**, 151318, DOI 10.1016/j.cej.2024.151318.

[3] L. Wang, D. Li, Q. Li, Q. Pan, M. Zhang, L. Zhang, F. Zheng, Y. Huang, H. Wang, Q. Li, Ultrafine zns nanoparticles embedded in N-doped carbon as advanced anode materials for lithium ion batteries and sodium ion batteries, J. Alloy. Compd., 2022, **910**, 164783, DOI 10.1016/j.jallcom.2022.164783.

[4] T. Shi, Y. Yang, M. Yu, W. Zhang, X. Ning, N,S co-doped biomass hard carbon/ZnS composite as the anode material for high-rate sodium-ion batteries, J. Energy Storage, 2024, **99**, 113246, DOI 10.1016/j.est.2024.113246.

[5] Y. Jin, H. Seong, J.H. Moon, S.Y. Lee, S.K. Kim, M. Yang, J.B. Lee, S.Y. Cho, J. Choi, Study on colloidal synthesis of ZnS nanospheres embedded in reduced graphene oxide materials for sodium-ion batteries and energy storage mechanism, J. Alloy. Compd., 2023, **943**, 169076, DOI 10.1016/j.jallcom.2023.169076.

[6] Y. Hao, Y. Cui, J. Wang, A. Li, F. Li, S. Yang, Interface engineering-induced enhancements in sodium-ion batteries: A nexus of ZnS nanoparticles and reduced graphene oxide for augmented storage and conductivity, J. Alloy. Compd., 2024, **1009**, 176837, DOI 10.1016/j.jallcom.2024.176837.

[7] D. Yan, Y.V. Lim, G. Wang, Y. Shang, X.L. Li, D. Fang, M.E. Pam, S.A. Yang, Y. Wang, Y. Shi, H.Y. Yang, Unlocking rapid and robust sodium storage performance of zinc-based sulfide via indium incorporation, ACS Nano, **2021**, 15, 8507-8516, DOI 10.1021/acsnano.1c00131.

[8] C.C. Li, B. Wang, D. Chen, L.-Y. Gan, Y. Feng, Y. Zhang, Y. Yang, H. Geng, X. Rui, Y. Yu, Topotactic transformation synthesis of 2d ultrathin GeS_2 nanosheets toward high-rate and high-energy-density sodium-ion half/full batteries, ACS Nano, 2019, **14**, 531-540, DOI 10.1021/acsnano.9b06855.

[9] X. Ou, Z. Xiao, J.F. Zhang, C. Wang, D. Wang, B. Zhang, Y. Wu, Enhancing the rapid Na^+-storage performance via electron/ion bridges through GeS_2/graphene heterojunction, ACS Nano, 2020, **14**, 13952-13963, DOI 10.1021/acsnano.0c06371.

[10] G. Xi, T. Zeng, Carbon confined GeS_2 particles and its three-dimensional flexible electrode toward sodium ion battery anode, J. Alloy. Compd., 2023, **937**, 168505, DOI 10.1016/j.jallcom.2022.168505.

[11] C. Wang, D. Wang, X. Ma, H. Qin, M. Liu, Y. Yan, B. Zhang, X. Ou, Isotropy-induced stress relaxation and strong-tolerance for high-rate and long-duration sodium storage by amorphous structure engineering, Adv. Funct. Mater., 2022, **32**, 2204687, DOI 10.1002/adfm.202204687.